The Synchronic Frame of Photospheric Magnetic field: The Improved Synoptic Frame

X. P. Zhao, J. T. Hoeksema and P. H. Scherrer
W. W. Hansen Experimental Physics Laboratory, Stanford University

Short title: SYNCHRONIC FRAMES

Abstract.

It is shown that because of the effect of the differential rotation, the magnetic elements in a Carrington synoptic map can not be used to fill up the entire solar surface at any time within the period of one solar rotation. By correcting the effect of the differential rotation included in synoptic maps, we improve the synoptic map to obtain the "synchronic map" as a proxy of entire solar surface distribution of the photospheric magnetic field. We further improve the synoptic frame by combining the synchronic map with the remapped magnetogram to obtain the "synchronic frame". The coronal holes and the base of the heliospheric current sheet reconstructed using the synchronic frame appear to be better than that using the synoptic frame, showing that the synchronic frame is a better proxy than the synoptic frame for the instantaneous entire surface distribution of the photospheric field at the time of interest.

1. Introduction

The classic "magnetic synoptic chart" (Bumba and Howard, 1965), was made from consecutive daily remapped magnetograms. Each remapped magnetogram (see the top panel of Figure 1) observed at its central meridian passing (CMP) time corresponding to a "Carrington longitude" is sliced a strip centered at the central meridian, and all obtained strips are ranged from right to left in the order of time or from left to right in the order of the Carrington longitude (see top and bottom labels of the middle panel). Since magnetic features rotate differentially depending on the latitude the magnetic features are located, the magnetic synoptic charts mix, in fact, the time and space. By implicitely neglecting the difference between the heliographic longitude and the Carrington longitude, the magnetic synoptic charts have usually been called "magnetic synoptic maps" (e.g., Harvey et al., 1980), i.e., considered as a proxy of the entire-photosphere distribution of the magnetic field, and surved as an inner boundary condition for various data-based coronal models. The successful reconstruction of coronal holes (Levine, 1975) and the base of the heliospherical current sheet (Hoeksema et al, 1983) strongly suggests that it is the directly underlying photospheric magnetic field that mainly responses for the overlying large-scale coronal structures.

Attemps have been made to obtain better representation of the entire solar surface distribution of the photospheric magnetic field.

Based on the high-cadence, high-resolution MDI magnetograms that can be reduced to low-cadence, low-resolution magnetograms with low noise at the time of interest (the target time hereafter), the "synoptic frame" has been developed to track the change of large-scale coronal structures on the time scale much less than one solar rotation period (Zhao, Hoeksema and Scherrer, 1997). As shown in Figure 1, the synoptic frame consists of two components: the target-time remapped magnetogram component and the synoptic map component. The remapped magnetogram with central meridian angles of $\pm 50^\circ$ covers most part of the Earth-side solar surface and avoids geometrical

factors that systematically bias the measurement. This component is expressed using the heliographic coordinate (See the red rectangular area in the top and bottom panels of Figure 1). The synoptic map component expressed by the Carrington coordinate is in the east and west parts of the synoptic frame which covers the unobserved farside and poor-observed Earth-side solar surface. To emphasize the major role played by the remapped magnetogram component (that is underlying the interesting coronal structure) in approximating the instantaneous entire surface field distribution and in tracking transient large-scale coronal structures, the term of "synoptic chart" or "synoptic map" is replaced by the term of "synoptic frame". The temporal variation of the 1996 August boot-shaped coronal hole boundary on the time scale of a day and the temporal variation of the 1994 April Soft X ray arcade on the time scale less than a day have been successfully reproduced using synoptic frames and various coronal magnetic field models (Zhao, Hoeksema and Scherrer, 1999; 2000). The successful modeling suggests that the synoptic frame is a better proxy than magnetic synoptic maps in representing the instantneous entire surface distribution of the photospheric field. However, as shown in the bottom panel of Figure 1, there is a mapping inconsistence in synoptic frames: the heliographic longitude in the magnetogram part and the Carrington longitude in the synoptic map part.

Recently, the "snapshot heliographic map" is developed (Ulrich and Boyden, 2006. UB06 hereafter) that removes the mixing between space and time in magnetic synoptic maps.

The present work tries to improve the synoptic frame by removing the mapping inconsistence so that the improved synoptic frame becomes true entire solar surface distribution of the photospheric field.

As discussed in UB06, the differential rotation may introduce errors into the magnetic synoptic maps in two ways. The first error is the differentially heliographic longitude shifts of magnetic elements between their observational time and the target

time due to the difference between magnetic feature's differential rotation rate and the Carrington rotation rate. The second is the smearing produced in merging and averaging over multiple strips. In Section 2, we will quantitatively examine the two errors in MDI and HMI synoptic maps and describe the way to remove the errors in MDI and HMI synoptic maps. We then construct the improved synoptic map that is called the "synchronic map" in what follows (which is similar to the MWO snapshot heliographic map). By merging the remapped magnetogram with the synchronic map to obtain the improved synoptic frame, the "synchronic frame". To see the effect of differential rotation on the entire surface distribution of the field strength and polarity structures, we compare the synchronic frame with the synoptic frame in Section 3. In Section 4 we show the effect of differential rotation on modeled coronal structures by comparing the coronal structures obtained using synchronic frames with that using synoptic frames, and by comparing the calculated results with observations. In the last section we summary the results and discuss the possibility of further improving the synchronic map and synchronic frame.

2. Effect of differential rotation on locating magnetic elements

Because of the differential rotation of photospheric magnetic features, the heliographic longitude of all magnetic elements over entire solar surface is time-dependent, except those their differential rotation rate is the same as the solar sidereal rotation rate. In other words, the entire solar surface distribution of the photospheric field is time-dependent. Any entire solar surface distribution of the photospheric field must be with respect to a reference time.

We set here the target time, say 1998:05:23_16:03:30, as the reference time, and the value of the Carrington longitude corresponding to the target time, 202° (for completeness, 1936 : 202°, here 1936 is the Carrington rotation number), as the value of the reference heliographic longitude, expressed as 1998.05.23 : 202°. This reference

heliographic longitude is located in the center of the heliospheric map. In this way, all magnetic elements on the entire solar surface at the target time will be distributed along meridians extend from 1998.05.23 : 022° at east side to 1998.05.23 : 022° at west side, as shown in the top panel of Figure 1. This heliographic grid system may regidly rotate as time goes on, and each central meridian observed at CMP time is expressed as a Carrington longitude with the same value as the value of the corresponding heliographic longitude at the reference time. In other words, for a magnetic element, its heliographic longitude at a time will or would be different from its heliographic longitude at the reference time. The change in heliographic longitude depends on the time difference and the helographic latitude of the magnetic element. Therefore, based on magnetic synoptic maps to constrauct an entire solar surface distribution of the photospheric magnetic field at a reference time t_r, it is necessary to first find out its observational CMP time from the Carrington longitude of the meridian where a magnetic element is located, and then calculate the change of its heliographic longitude using the difference of its observational time from the reference time, its latitude, the differential rotation rate and the solar rotation rate.

2.1. Inversion of Carrington longitude to CMP time

If Carrington longitudes are calculated from CMP times using a constant synodic rotation period of 27.2753 days during the constraction of synoptic maps, the time difference between Carrington longitudes, say between 1936_27° (1936_182°) and 1936_202°, can be easily calculated to be 318.21 (36.37) hours, and the time difference is independent of Carrington rotation number, as shown by the blue lines in Figure 2. The algorithm used in UB06 is based on the constant synodic rotation period.

The Carrington longitude is usually calculated from CMP times taking into consideration of the eccentricity of the Earth's orbit, and the synodic rotation period varies during a year. The time difference mentioned above would depend on the

Carrington rotation number too. In the WSO software system of the Stanford Solar Physics Group, there is a code, "times", that is used to carry out the conversion between the CMP time and the Carrington longitude. The code is developed about 20 years ago on the basis of ephemeris algorithm, and introduced a parameter called "Carrington time" that was expressed as, for example, "CT1936:201.74" for the Carrington longitude of 201.74° at Carrington number of 1936. We improve the code recently to more accurately carry out the conversion. The error of such inverted CMP time from the true CMP time is only about 15 second. The red curves in Figure 2 denote the time difference calculated using the same given Carrington numbers and Carrington longitudes as the case of the blue lines. The annual variation of the red curves is consistent with the annual variation of the synodic rotation period. Figure 2 shows that the effect of varying synodic rotation rate may not be neglected when the separation of two Carrington longitudes significantly greater than 50°, especially around solstices.

2.2. The shift in heliographic longitude of magnetic elements

The differential rotation of solar features, such as spots, plages, and magnetic network, have been studied extensively, and various methods and data selection have led to different rotation rates. These differences have long been interpreted in terms of anchoring depth of different features (Meunier, 2006).

The synodic rotation rate of photospheric magnetic features is latitude-dependent and usually expressed as

$$\omega(\lambda) = A + B\sin^2(\lambda) + C\sin^4(\lambda) \tag{1}$$

where λ denotes the heliographic latitude of magnetic elements. The coefficients A, B and C vary depending on the selected magnetic feature and analytic method (e.g., Liu and Zhao, 2009 and references therein). We tried a few sets of the coefficients, and found that the widely-used Snodgrass (1983) rotation rate is equal to the Carrington

rotation rate, as expected, at the heliographic latitude of $\pm 16°$, and the coronal holes predicted from the synchronic frame obtained using this differential rotation rate agree with observation better than other rotation rates. In the following calculation, we use Snodgrass rotation rate, i.e., $A = 13.3445$, $B = -1.56154$, and $C = -2.23407$ in deg/day.

After calculating the time difference of every Carrington longitude in a synoptic map from the reference time, the shift in heliographic longitude each magnetic element subjected can be estimated based on the latitude of the element and Equation (1). The second panel in Figure 3 shows the effect of the differential rotation on the heliographic longitude of magnetic elements. The red vertical line in the center of the all panels denotes the Carrington longitude of 1936:202° which corresponds to the target time of 1998.05.23_16:03:30 and the reference heliographic longitude of 1998.05.23:202°. The blue vertical lines in the top two panels denote the Carrington longitudes corresponding to CMP times other than the reference time. The time difference of the blue vertical lines from the central red vertical line can be calculated mentioned above. Each black or red curve is the locus of heliographic longitudes calculated using the time difference for all magnetic elements along the meridian. The two horizontal lines in the second panel denote locus of latitudes where the differential rotation rate equals the Carrington rotation rate. The longitudinal difference of a curve from the vertical blue line that intersects the curve denotes the heliographic longitude shift of the magnetic elements.

As shown in the panel, there are four corners within the 1936:202°-centered non-traditional synoptic map bound at 1935:022° and 1936:022°, where no black curve occurs, demonstrating that the magnetic elements in the non-traditional synoptic map (in fact, any synoptic map) cannot be used to completely fill up the entire solar surface at any instant within the period of the rotation.

As expected, the longitude shift depends on the latitude of magnetic elements and the distance of each blue line from the central red line. For the distance greater than 50°,

a shift of 10° occurs at most of latitudes above ±16∘, indicating the significant effect of the differential rotation included in the synoptic map component of the synoptic frmae.

2.3. Examination of smearing occurred in averaging over multiple observed strips

The Sun's differential rotation may also cause smearing occurred in merging and averaging over multiple observed strips of remapped magnetograms, as pointed out in UB06. For each strip observed at its CMP time, except the central meridian line that is expressed by Carrington longitude corresponding to the CMP time, other meridian lines in the strip may be expressed by central meridian angles or heliographic longitudes with respect to the same CMP time. To avoid the smearing it is necessary to convert these heliographic longitudes at same CMP time to their apparent Carrington longitudes (or CTELs in UB06) corresponding to varios times different from the CMP time. The blue curves in the third panel of Figure 3 are the locus of calculated apparent Carrington longitudes. Each blue curve intersects a vertical black line at two latitudes where the differential rotation rate equals the Carrington rotation rate. The angular shift of a blue curve from its intersected black vertical line depends on the central meridian angle of the black line from the red line and the latitude of magnetic elements. As shown in the panel, for the black lines at central meridian angles greater than |20°|, the angular shifts are significant for latitude greater than |30°|. On the other hand, for the black lines at central meridian angles less than |10°|, the angular shifts are undetectable for latitude less than |55°|, and the shifts are only a couple of degrees at latitude higher than |75°|. Therefore, the smearing depends on the central meridian angle or the width of strips that are used to build magnetic synoptic maps.

For magnetic synoptic maps of daily magnetograms, the smearing is significant because the centrial meridian angle of strips is greater than |20°|, as shown in UB06. However, for magnetic synoptic maps of 96-min (MDI) or 12-min (HMI) magnetograms,

the smearing is negligible because the central meridian angle of strips is less than $|10°|$ (it is only 9° for MDI and 1.5° for HMI). We will correct the effect of differential rotation included in magnetic synoptic maps only by removing the inconsistent mapping in next section.

3. Construction of magnetic synchronic maps and synchronic frames

As mentioned above, the magnetic elements included in a magnetic synoptic map can not be used to fill up entire solar surfacebe at any time in the solar rotation. To cover entire solar surface, more observational data than over one solar rotation are needed. For the target time of 1998.05.23_16:03:30, i.e., the red vertical lines in Figure 3, the magnetic elements along the red curves in the right (left) quadrant that are observed at times between Carrington longitudes of $1935 : 112°$ and $1935 : 022°$ ($1936 : 22°$ and $1937 : 292°$) are needed for filling up the right (left) blank corners of black curve in the synoptic map (see the first and second panels of Figure 3).

The magnetic field distribution will be changed because of the shifts of heliographic longitudes relative to their original meridian line. To obtain the magnetic field distribution in heliographic coordinates, we displace magnetic elements at each blue vertical line (see the first panel) to corresponding red or black curves (see the second panel) and then get the neuboring averages of the moved magnetic elements at the same latitude around each heliographic longitude.

The bottom panel of Figure 3 shows the MDI magnetic synchronic map, the same as the "Snapshot heliographic map" in UB06. It centers at the heliographic longitude of 1998.05.23:202.°, as shown by the vertical red line and obtained using data of the extended synoptic map (the first panel). It can be considered as the instantaneous magnetic field distribution over the entire solar surface at the time of 1998.05.23_16.03.30

if the evolution of the photospheric magnetic field in the period of time is caused purely by the differential rotation.

The synchronic frame (as shown in the second panel of Figure 6) is thus obtained by merging the remapped magnetogram (the top panel of Figure 1) with the synchronic map (the bottom panel of Figure 3).

4. The effect of differential rotation on the distribution of the field strength and polarity structures

To see if the technique developed here works we first compare the field strength distribution between the synchronic map and synoptic map.

Figure 4 displays the longitudinal variation of magnetic field strength at latitudes of $-84°$, $-60°$, $-30°$, $-16°$, and $0°$. The blue (red) lines in all panels denote the longitudinal variation in the synchronic (synoptic) maps. As expected, there is no shift between the blue and red lines at latitude of $-16°$, where the differential rotation rate is the same as the Carrington rotation rate. Above (below) the latitude of $16°$ the blue line significantly shifts, relative to the red line, toward (away from) the central black vertical line from two sides. The shift increases as the heliographic longitude aways from the central black vertical line and as the latitude increases.

The effect of the differential rotation on large-scale magnetic polarity distributions should also be detectable. Figure 5 shows a quantitative sketch of the effect. The rectangles bound by thick (thin) line denote the areas occupied by magnetic structures in the synchronic map (synoptic map). Depending on the latitude and the longitudinal distance from the center, the thick line rectangles, relative to the thin line rectangles, displace toward the center with their upper parts shear more than the lower parts and their rear parts move more than front parts.

Such differences are perceptible in the bottom panel of Figure 3. All active regions

away from the red line in the panel show a displacement toward the red line with respect to the top panel. For instance, the active regions located at $\pm 30^\circ$ of latitude and 1998.05.23_350° of longitude moved about 5° leftward relative their counterpart in the bottom panel of Figure 1. In addition, the active region in northern (southern) hemisphere in the bottom panel of Figure 3 shows a slight counter clock-wise (clock-wise) rotation with respect to the bottom panel of Figure 1. The structures in the east side shows an opposite rotation. This tendency of rotation is consistent with Figure 5.

5. Effect of differential rotation on modeled coronal structures

To see the Effect of differential rotation correction on modeled coronal structures, we compute the open field regions and the source surface neutral line by inputing the synchronic and synoptic frames into the potential field-source surface model.

The top two panels of Figure 6 are the synoptic and synchronic frames. Overplotted are the photospheric polarity inversion lines of large-scale field (green curves). Between the two panels, differences like those found in Figures 4 and 5 also appear in the frames outside the rectangle bound by dashed lines. The displacing, tilting and shrinking of the positive (white) and negative (black) regions in the second panel indicate the effect of the differential rotation on the distribution of magnetic polarity structures.

What is the effect of this difference on the calculated coronal field, specifically, on modeled coronal holes and the base of the heliospheric current sheet (HCS)?

The bottom two panels of Figure 6 display positive and negative (blue and red) open field regions, the source surface field strength distribution (see contours in grey images) and the neutral lines (black curves). The source surface is located at 2.5 solar radii and the principal order of the spherical harmonic series used in the calculation is 45. The green line in the bottom panel is the same as the neutral line in the third panel. The difference between the two neutral lines in the bottom panel is caused by the correction of differential rotation. The difference of calculated coronal holes between

the two panels are also evident both in the portion outside the the rectangle and within the rectangle.

Figure 6 shows that although the correction changes the photospheric field distribution only in the synoptic map component, i.e., the portion outside the rectangle, calculated coronal holes and the HCS are changed in the portion within the rectangle as well as in the portion outside the rectangle.

To see whether or not the magnetic synchronic frame represents a better instantaneous whole surface distribution of the photospheric magnetic field than the synoptic frame, it is necessary to compare the modeled coronal and heliospheric structures overlying the rectangle with observations made at the same time.

Since the synchronic frame is supposed to be a better proxy for the global distribution of the photospheric field at the target time, the coronal structure and the HCS to be compared must be observed near the same time.

The outlines in Figure 7 show the boundary of 1083 nm coronal holes observed at 1998.05.23_17:13 by the NSO Vacuum Telescope of the Kitt Peak Observatory. It is shown that both the blue and red foot point areas calculated using synchronic frame cover larger polar hole area than that using the synoptic frame, though the improvement is not dramatic. That the improvement is not dramatic may be understood because the modeled coronal hole is governed mainly by its underlying magnetic field and what is corrected is the magnetic field not underlying the coronal hole.

6. Summary and Discussion

We have shown that the magnetic elements from a Carrington synoptic map cannot be used to fill up the whole solar surface at any time within the Carrington rotation period because of the differential rotation of magnetic features. To fill up the whole solar surface at a specific time 41 days (one and half solar rotation periods) of observations are needed.

We have shown that the smearing in averaging over multiple strips is heavily dependent on the central meridian angle of the strips. For high-cadence magnetograms, such as MDI and HMI, the central meridian angle is less than 10°, the smearing is negligibal.

By converting Carrington longitudes in magnetic synoptic maps to heliographic longitudes with respect to a reference time we construct the MDI synchronic map. By replacing the central part of the synchronic map with the remapped magnetogram at the same time, we obtain the improved synoptic frame, the "synchronic frame".

The comparison of modeled coronal holes and the heliospheric current sheet obtained using the synoptic frame with that using the synchronic frame shows detectable changes in the modeled coronal structures. It is further shown that the modeled coronal holes using the synchronic frame agree with observation of coronal holes better than using the synoptic frame. The results show that the effect of differential rotation on the surface distribution of photospheric magnetic field should be corrected in constructing the instantaneous entire surface distribution of magnetic fields. The simultaneously observed different coronal and heliospheric structures located, respectively, underlying spacecraft SOHO, SDO, and the STEREO A and B will be used to further test the synchronic frame.

The evolution of the photospheric magnetic field depends on other ingredients as well as the differential rotation. Flux transport models that incorporates flux emergence, random-walk dispersal, meridional advection, differential rotation, and removal of flux via cancellation (Schrijver and Derosa, 2003, and references therein), can be used to simulate the evolution of the photospheric magnetic flux from instant to instant over the whole solar surface. The Flux transport models need an initial, instantaneous whole surface distribution of the photospheric magnetic flux as an seed input. The magnetic synchronic frame is a better input to the models than the magnetic synoptic map. What predicted from the models and the magnetic synchronic frame is expected to be closer

to the realistic whole-surface distribution than what from the magnetic synoptic map.

7. Acknowledgments

References

Bumba, B. and R. Howard, *Astrophys. J., 141*, 1502, 1965.

Harvey, J., Gillespie, B., Meidaner, P., and Slaughter, C., *World Data Center Report, UAG-77*, 1980.

Hoeksema, J. T., J. M. Wilcox, and P. H.Scherrer, *J. Geophys. Res., 88*, 9910, 1983.

Levine, R. H., *Solar Phys., 51*, 345, 1977.

Liu, Y. and J. Zhao, Solar Physics, 260(2), 289, 2009.

Meunier, N., *Astron. & Astrophys., 436*, 1075, 2005.

Schrijver, C. J. and DeRosa, M. L., *Solar Physics, 212*, 165, 2003.

Ulrich, R. K. and J. Boyden, *Solar Phys., 235*, 17, 2006.

Zhao, X. P., J. T. Hoeksema, P. H. Scherrer, *The Proceedings of the Fifth SOHO Workshop at Oslo*, SH-404, p. 751, 1997.

Zhao, X. P., J. T. Hoeksema, P. H. Scherrer, *J. Geophys. Res., 104*, p. 9735, 1999.

Zhao, X. P., J. T. Hoeksema, P. H. Scherrer, *Astrophys. J., 538*, 932, 2000.

X. P. Zhao, W. W. Hansen Experimental Physics Laboratory, Stanford University, Stanford, CA 94305-4085. (e-mail: xuepu@quake.stanford.edu)

J. T. Hoeksema, W. W. Hansen Experimental Physics Laboratory, Stanford University, Stanford, CA 94305-4085. (e-mail: jthoeksema@solar.stanford.edu)

P. H. Scherrer, W. W. Hansen Experimental Physics Laboratory, Stanford University, Stanford, CA 94305-4085. (e-mail: phscherrer@solar.stanford.edu)

Received _____

Second Version:15 Jul. 2011

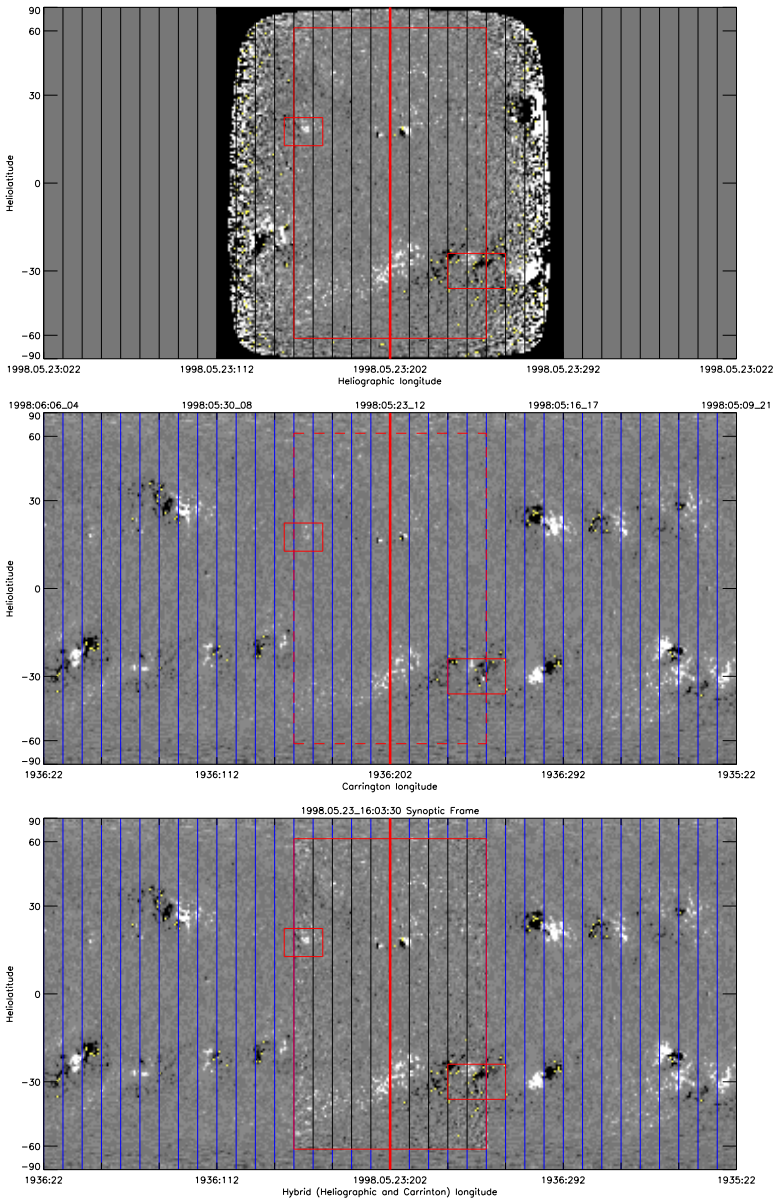

Figure 1. Construction of the synoptic frame of the photospheric magnetic field (bottom panel) using a remapped magnetogram (top panel) and an non-traditional synoptic chart (middle panel). Black and blue vertical lines denote, respectively, Heliographic and Carrington longitudes. The abscissa in bottom panel is in hybrid manner, using heliographic longitude for magnetogram component, and using Carrington longitude for synoptic chart component.

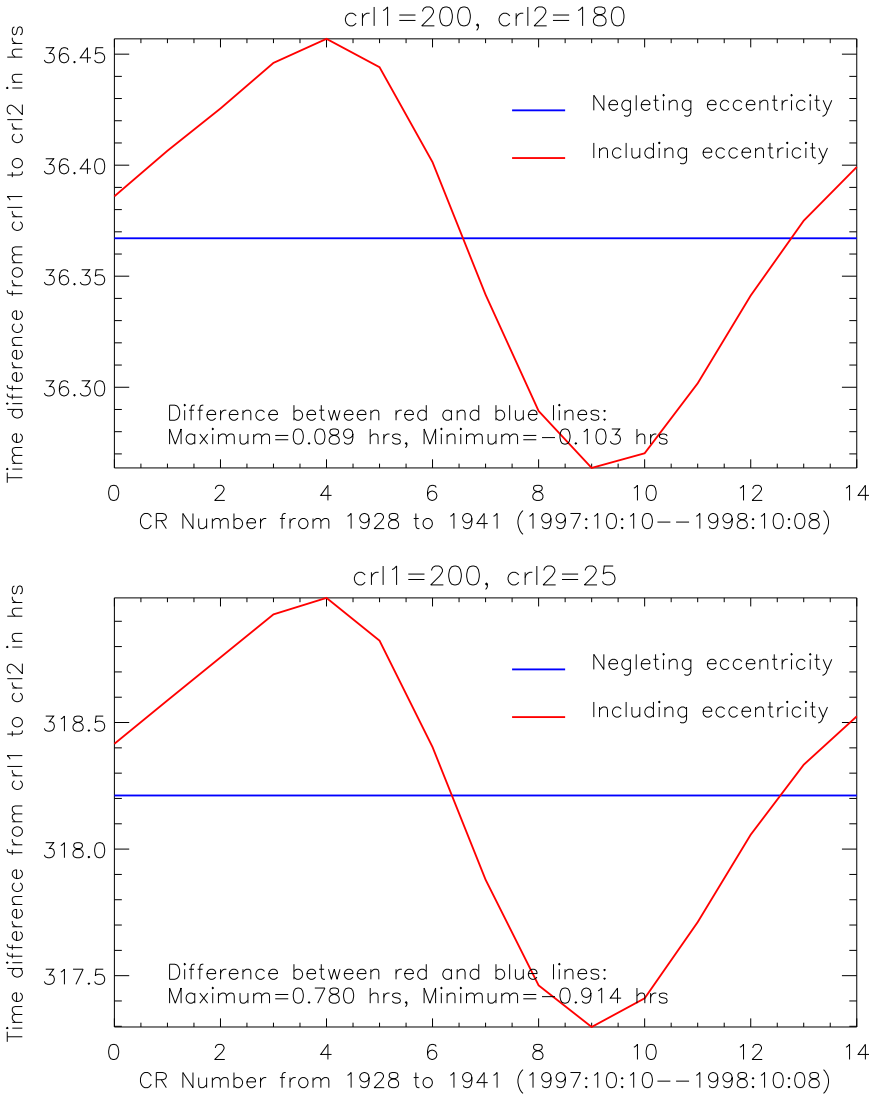

Figure 2. Comparison of time differences converted using two methods. The red curve is obtained using the code taking consideration the eccentricity of the Earth's orbit and the blue line is obtained using the code neglecting the eccentricity of the Earth's orbit.

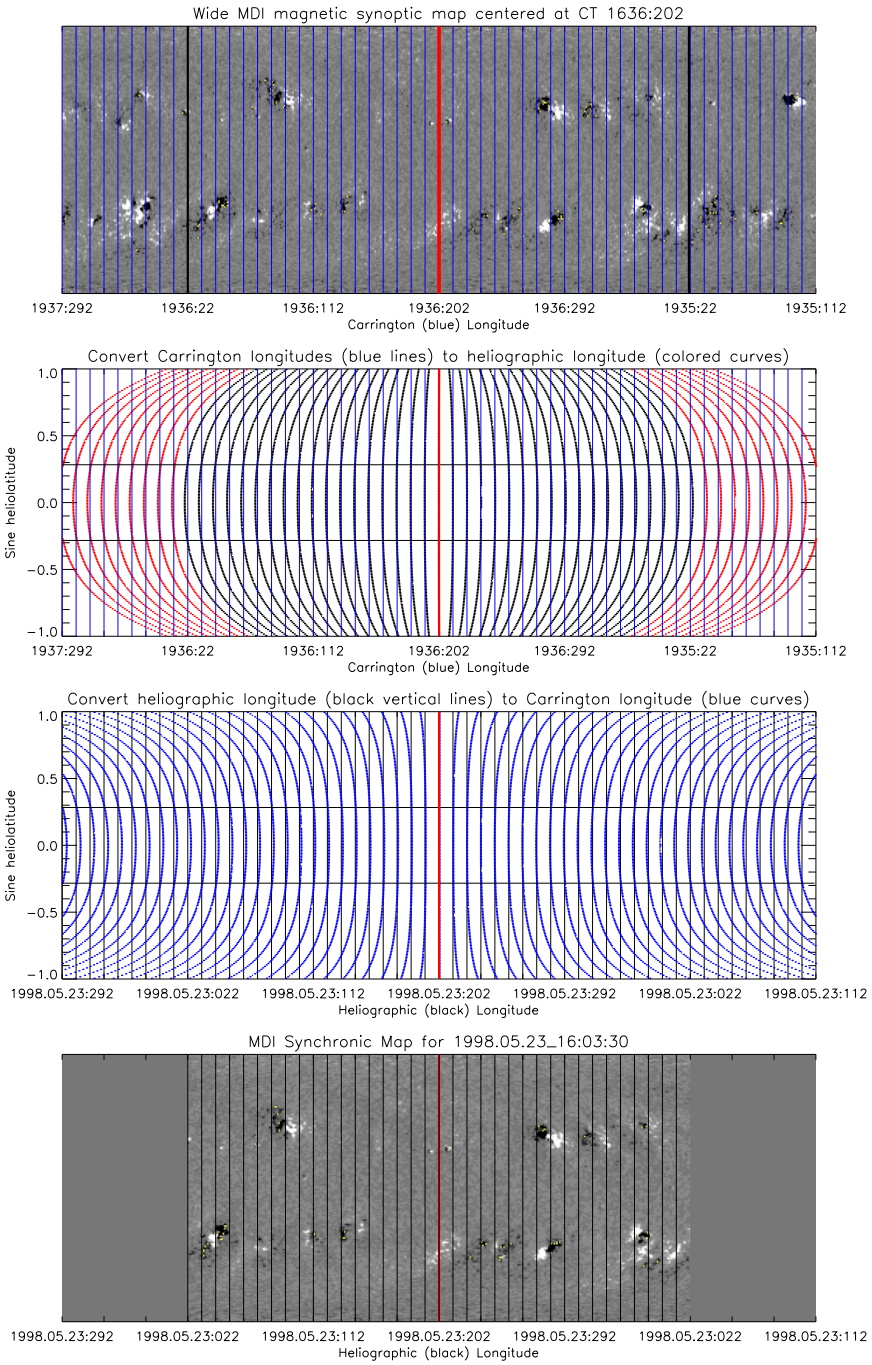

Figure 3. Construction of synchronic charts (bottom panel) from non-traditional synoptic charts (top panel). The abscissa in top (bottom) panel is in Carrington (Heliographic) longitude (see text for details).

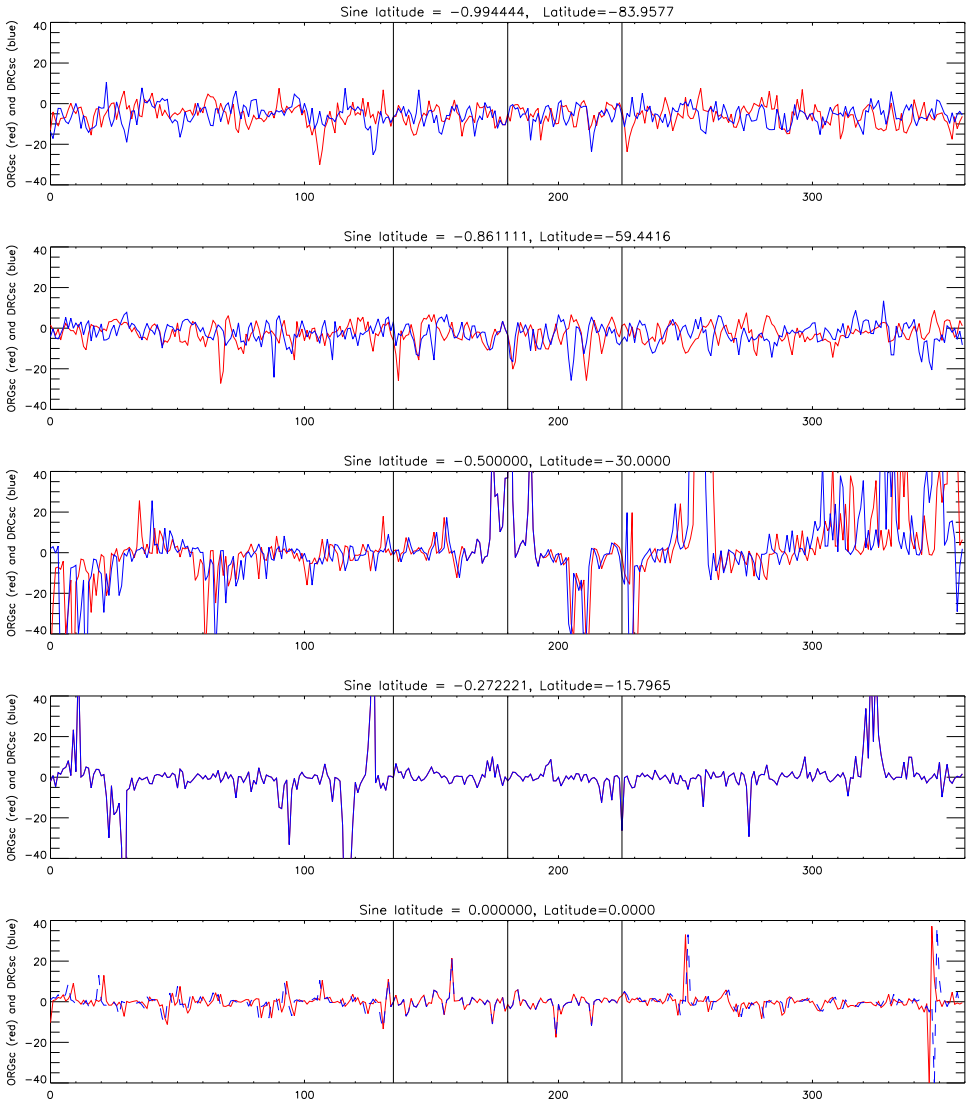

Figure 4. Comparison of the longitudinal variation of magnetic field at latitudes of 0, 16, 30, 60 and 84° (from bottom to top) between the synoptic chart (red lines) and the synchronic map (blue lines).

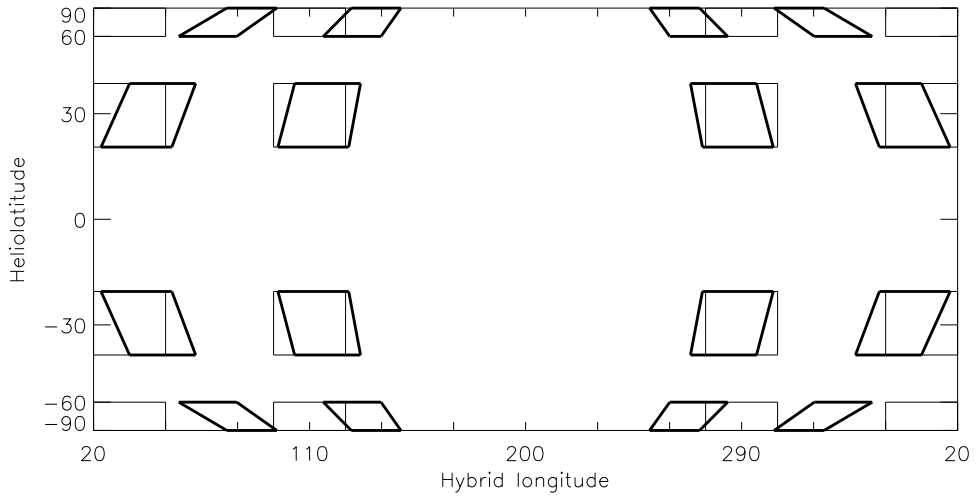

Figure 5. Comparison between non-traditional synoptic charts (thin outlines) and synchronic charts (thick outlines), showing the effect of differential rotation on magnetic structures.

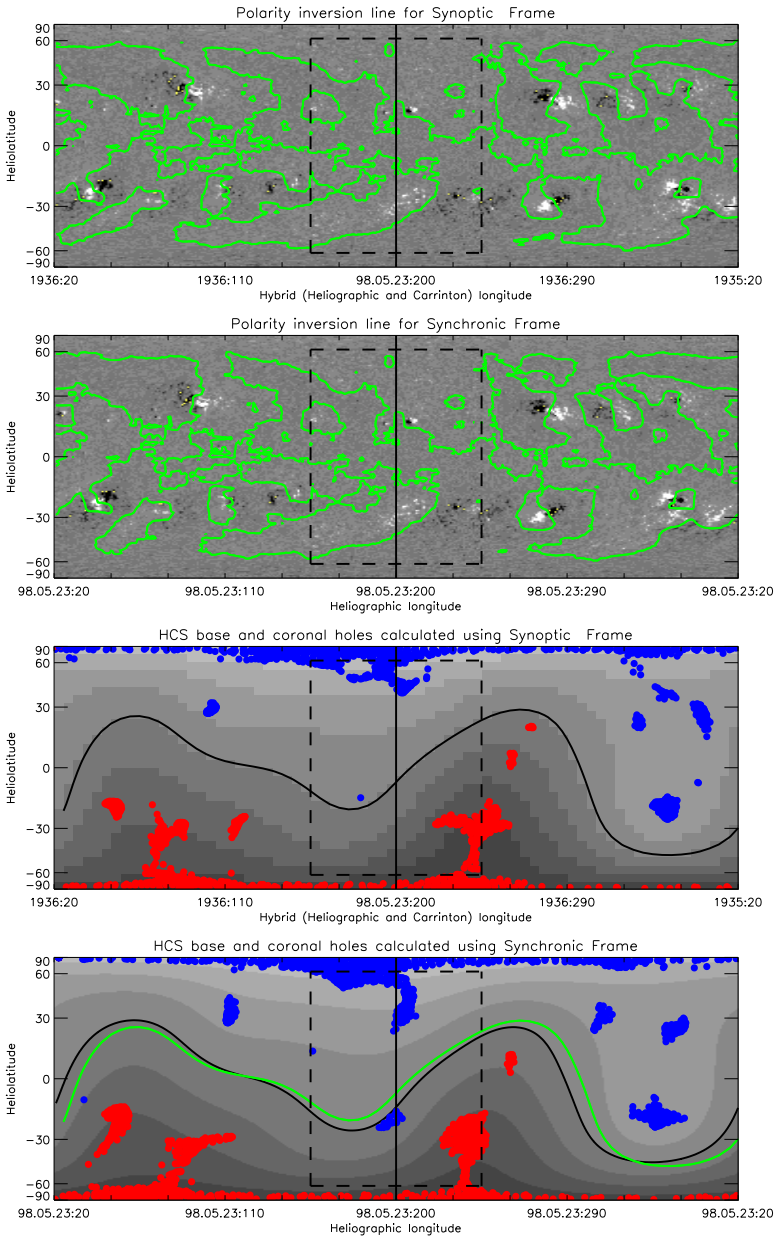

Figure 6. Comparison between synoptic frames (the first panel) and synchronic frame (the second panel). The green lines in the two panels are polarity inversion lines of large-scale photospheric field. The third and fourth panels shows the foot-points of open field lines (blue-positive and red-negative) and source surface neutral lines calculated using the first and second panels, respectively.

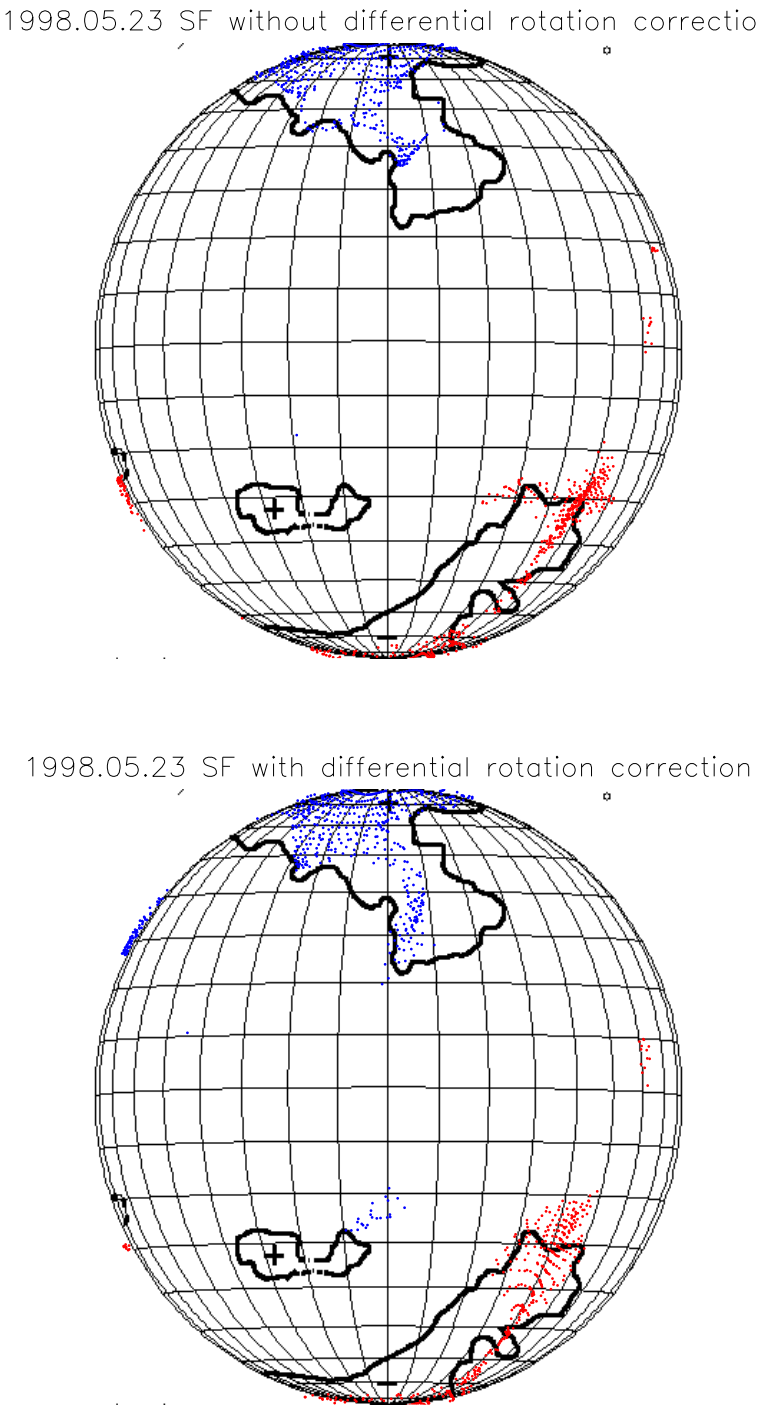

Figure 7. Comparison of open field regions calculated using the 1998.05.23_16:03:30 synoptic frame and the synchronic frame with KPNO He 1083.0 nm coronal holes observed at 1998.05.23_17.43.